

## Chapter 12

# Morphological Continuity of the Face in the Late Middle and Late Pleistocene Hominins from Northwestern Africa: A 3D Geometric Morphometric Analysis

K. Harvati and J.-J. Hublin

**Abstract** Facial morphology comprises some of the most distinctive features of early modern humans. The rich fossil record of Morocco allows assessing changes in facial morphology from the late Middle Pleistocene through the Late Pleistocene. Specimens associated with the Aterian industry in Morocco were originally thought to be relatively recent (40–20 ka), but could be much older (35–90 ka). Predating this population are the late Middle Pleistocene specimens of Irhoud. Later in the same geographical area, larger samples are represented by the Iberomaurusian series. We conducted a 3D geometric morphometric analysis of the facial shape of the Aterian specimen Dar es-Soltan II-5, with the aim of deciphering the affinities of this specimen with earlier North African and Levantine fossils, later Upper Paleolithic Eurasian specimens, as well as later North African populations. We used a large comparative sample ( $n = 191$ ) comprising seven geographic populations of recent humans, Iberomaurusians from Afalou and Taforalt ( $n = 22$ ), and Middle and Late Pleistocene Eurasian and African fossils. The 3D coordinates of 19 facial landmarks were collected. Specimen landmark configurations were processed with Generalized Procrustes Analysis. Principal Components, Canonical Variates, and cluster analyses were performed and Procrustes distances and Mahalanobis squared distances were calculated. Both Irhoud 1 and Dar es-Soltan II-5 are similar to the early anatomically modern humans from Qafzeh, and the Iberomaurusian sample is closely connected to the Upper Paleolithic European sample.

**Keywords** Aterian • Facial morphology • Modern human origins • Neandertals • Upper Paleolithic

## Introduction

Northwestern Africa has yielded a rich series of human fossils documenting human evolution throughout the Middle and Late Pleistocene (e.g., Hublin 1985, 1992, 2001). Recent developments in the determination of a secure chronology for the North African fossil record have raised new questions about the role of this area in the emergence of our species and the origins of non-African modern humans. Specifically, the Aterian assemblages that yielded robust modern looking human remains (Ferembach 1976) and which were initially assigned to a period between 40 and 20 ka (e.g., Debénath et al. 1986) are now considered to be much older. The bulk of the Aterian industries is likely to be dated between 90 and 35 ka and could well be rooted further back in time during the MIS 6 (see Bouzouggar and Barton 2012; Raynal and Occhietti 2012; Richter et al. 2012). Among the Aterian sites that have yielded fossil hominins, the cave of Dar es-Soltan II, near Rabat (Morocco), is best known for the rather complete cranial elements (a partial skull and the associated mandible) discovered in the site (Debénath 1976; Ferembach 1976). The specimen generally reported as Dar es-Soltan 5 was discovered under a sandstone plate within the marine sand deposits at the bottom of the stratigraphic sequence of the site (layer 7). For the purpose of clarity, it is designated here as Dar es-Soltan II-5. This archaeologically sterile layer was overlaid by a distinct reddish layer (layer 6) where a hearth and some Aterian elements have been described (Debénath 1976). Racemization ratios in molluscs from layer 7 indicate an age between 85 and 75 ka (Raynal and Occhietti 2012), compatible with other Aterian dates recently established in northern Africa.

---

K. Harvati (✉)

Senckenberg Center for Human Evolution and Paleoecology,  
Institut für Ur- und Frühgeschichte und Archäologie des  
Mittelalters, Eberhard Karls Universität Tübingen,  
Rümelinstraße 23, 72070 Tübingen, Germany  
e-mail: katerina.harvati@ifu.uni-tuebingen.de

J.-J. Hublin

Department of Human Evolution, Max Planck Institute for  
Evolutionary Anthropology, Deutscher Platz 6,  
04103 Leipzig, Germany  
e-mail: hublin@eva.mpg.de



**Fig. 12.1** Dar es-Soltan II-5

In light of these developments, the issue of continuity between the Aterian remains and those of the later Iberomaurusians (dated to 20–10 ka) becomes critical as the chronological distance between the two series of fossil remains increases. Is there evidence of morphological affinities, suggesting population history links and possibly a late chronology, between Dar es-Soltan II-5 and the Iberomaurusians? Or does the morphological evidence point to an evolutionary discontinuity and/or a large chronological gap in the human occupation record? Similarly, the relationship of the Aterians to the earlier specimens from Irhoud, dated to approximately 160 ka (Smith et al. 2007), also becomes relevant.

We conducted a 3D geometric morphometric analysis of the facial morphology of the Dar es-Soltan II-5 individual (Fig. 12.1) in comparison with the Jebel Irhoud and Iberomaurusian specimens, as well as with a large sample of recent humans, Neandertals and early modern humans from the Levant. Our goal was to evaluate the hypothesis of phylogenetic affinities among these fossil samples and, therefore, of continuity or discontinuity in North African human occupation. If there is a strong phylogenetic relationship and continuity among the North African fossil samples, it is expected that they will show greater similarity to older and younger specimens from the same region than to specimens from other parts of the world.

**Table 12.1** Recent human comparative sample

Total	( <i>n</i> = 213)
Sub-Saharan African (E. & S. Africa)	( <i>n</i> = 38)
Andaman Islanders	( <i>n</i> = 29)
Australian	( <i>n</i> = 26)
Asian (China, Thailand)	( <i>n</i> = 38)
Inuit (Alaska, Greenland)	( <i>n</i> = 14)
Near Eastern (Syria)	( <i>n</i> = 20)
European (Germany, Greece, Czech Republic, Norway)	( <i>n</i> = 25)

**Table 12.2** Fossil and subfossil samples included in the analysis

<b>Mid-Pleistocene Europe (MPE)</b>	( <i>n</i> = 3)
Arago 21, Petralona, Sima de los Huesos 5	
<b>Mid-Late Pleistocene Africa (MPA)</b>	( <i>n</i> = 3)
Bodo, Kabwe, Irhoud 1	
<b>Neandertals</b>	( <i>n</i> = 6)
Gibraltar 1, Shanidar 5, Guattari 1, La Chapelle, La Ferrassie 1, Shanidar 1	
<b>Late Pleistocene Near East</b>	( <i>n</i> = 2)
Qafzeh 6, Qafzeh 9	
<b>Late Pleistocene Eurasia</b>	( <i>n</i> = 14)
Chancelade, Abri Pataud 1, Cro-Magnon 1 & 2, Mladec 1, Predmost 3 & 4, Grimaldi 4, Upper Cave 101 & 103, Ohalo II	
<b>Late Pleistocene Africa</b>	( <i>n</i> = 1)
Wadi Kubbania	
<b>Iberomaurusian</b>	( <i>n</i> = 22)

## Materials and Methods

Our comparative sample comprised a total of 213 individuals from seven geographical samples of recent humans, which, together, span a large extent of the modern human geographic range (Table 12.1). It also included several Middle/late Middle Pleistocene fossil humans from Africa and Eurasia and a large Iberomaurusian sample from Afalou and Taforalt (Table 12.2). Nineteen facial osteometric landmarks were digitized using a Microscribe by one observer (KH) (Table 12.3, Fig. 12.2). Data were collected in the form of 3D coordinates, and processed with Generalized Procrustes Analysis. In cases of only minimal bone loss, missing data were reconstructed during data collection using anatomical clues from the preserved surrounding areas. Bilateral landmarks missing on one side were estimated during data processing by mirror-imaging using reflected relabelling (Mardia and Bookstein 2000; Gunz and Harvati 2007), which reflects the paired landmarks without having to specify a mirroring plane.

**Table 12.3** Facial landmarks digitized and their definitions

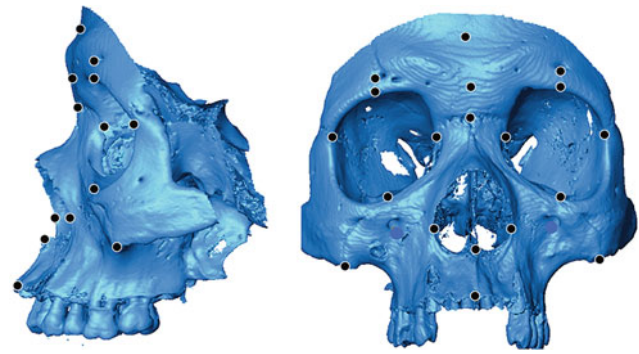
1. Post-toral Sulcus	Minima of concavity on midline post-toral frontal squama
2. Glabella	
3. Nasion	
4. Nasospinale	
5. Prosthion	
6, 7. Mid-orbit Torus Superior	Point on superior aspect of supraorbital torus, approximately at the middle of the orbit
8, 9. Mid-orbit Torus Inferior	Point on inferior margin of supraorbital torus, approximately at the middle of the orbit
10, 11. Dacryon	
12, 13. Zygoorbitale	
14, 15. Frontomalare Orbitale	
16,17. Zygomaxillare	
18, 19. Alare	

The superimposed coordinates were then analyzed using an array of multivariate statistics: Principal Components Analysis (PCA), Canonical Variates Analysis (CVA), Mahalanobis squared distances ( $D^2$ , corrected for unequal sample sizes following Marcus (1993)), Procrustes distances (PD), and cluster analysis with the Neighbor Joining Tree method.

In contrast to conventional linear and angular measurements, our coordinate-based approach preserves the geometry of the object studied and allows the intuitive visualization of shape differences between specimens or group averages as landmark displacements (Rohlf and Marcus 1993; O'Higgins 2000; Harvati 2001, 2003a, b). Geometric morphometric methods also provide a way of quantifying shape variability of traits that are difficult to measure with traditional measurement methods, and are therefore usually described qualitatively (Harvati 2001, 2003a; Nicholson and Harvati 2006).

## Results

**PCA:** The first PC (19.5% of total variance) reflects variation in facial morphology among all groups, with the Inuit samples separating somewhat from other groups on the negative end of this axis (Fig. 12.3). Specimens scoring negatively on this PC show supero-inferiorly tall and medio-laterally narrow faces, with more coronally oriented zygomatics and less subnasal prognathism compared to specimens scoring positively on PC 1. PC 2 (12.4% of total variance), in contrast, separates Neandertals and other “archaic” humans from

**Fig. 12.2** Facial landmarks digitized for this study

modern humans (Fig. 12.3). The Middle Pleistocene specimens from both Africa and Europe occupy an intermediate position: Kabwe, Arago, Sima 5, and Petralona place closer to the Neandertals, while Bodo is closer to modern humans and to the early anatomically modern specimens Qafzeh 6 and 9. Jebel Irhoud 1 is also close to the Qafzeh specimens and well within the recent human range of variation along PC 2, while Dar es-Soltan II-5 falls within the modern human cloud. The Iberomaurusians and Upper Paleolithic specimens from Eurasia and Africa are well within modern human variation on this axis. The shape differences along PC 2 include a heavier browridge, longer face, more projecting midface, more inflated maxilla, and more posteriorly sloping zygomatics on the Neandertal end (Fig. 12.3).

**CVA:** The CVA was calculated using the first 13 principal components (representing about 85% of the total variance). The first canonical axis accounts for 37.4% and separates archaic from modern humans (Fig. 12.4). Here, all the Middle Pleistocene specimens fall around the Neandertal cloud, with Bodo again occupying the most intermediate position. Qafzeh 6 and 9 fall very close to Bodo and to each other towards the modern human cloud. Irhoud 1 and Dar es-Soltan II-5 are very close to the Qafzeh individuals. They are intermediate to Neandertals/Middle Paleolithic European and African specimens on the one hand and modern humans on the other. As in the PCA, the Iberomaurusians and Upper Paleolithic specimens from Eurasia and Africa are well within the range of modern human variation.

**$D^2$ :** The Mahalanobis squared distances among groups are reported in Table 12.4. They were calculated on the basis of the first 13 principal components. Irhoud 1 was found to be closest to the Upper Cave specimens ( $d^2 = 1.91$ ) and to Qafzeh 9 ( $d^2 = 3.4$ ). Dar es-Soltan II-5 showed much larger overall distances to all groups included in the analysis. It was closest to Petralona ( $d^2 = 5.46$ ), to Qafzeh 6 and 9 ( $d^2 = 10.65$  and  $12.57$ , respectively), and to Wadi Kubbania ( $d^2 = 12.7$ ). The Iberomaurusian sample was closest to the European Upper Paleolithic sample

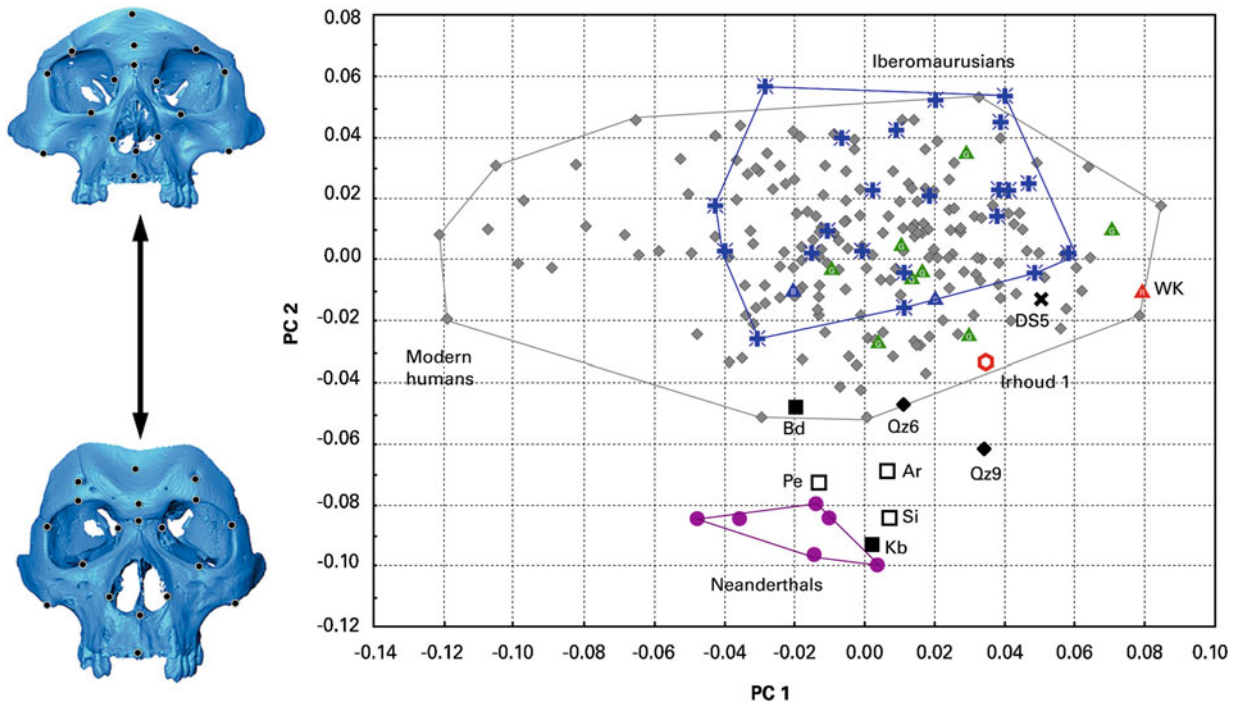


**Fig. 12.3** Principal components analysis. On the left side are shown the shape changes along PC 2 in frontal view. Symbols are as follows: Red star: Jebel Irhoud 1 (Irhoud1); Black star: Dar es-Soltan II-5 (DS5); Blue stars: Iberomaurusians; Purple dots: Neanderthals; Black squares: Bodo (Bd), Kabwe (Kb); Open squares: Arago (Ar), Sima 5

(Si), Petralona (Pe); Green triangles: Up. Paleolithic Europeans; Blue triangles: Upper Cave 101 and 103; Red triangle: Wadi Kubbaniya (WK); Black diamonds: Qafzeh 6 & 9 (Qz6, Qz9); Grey diamonds: recent humans

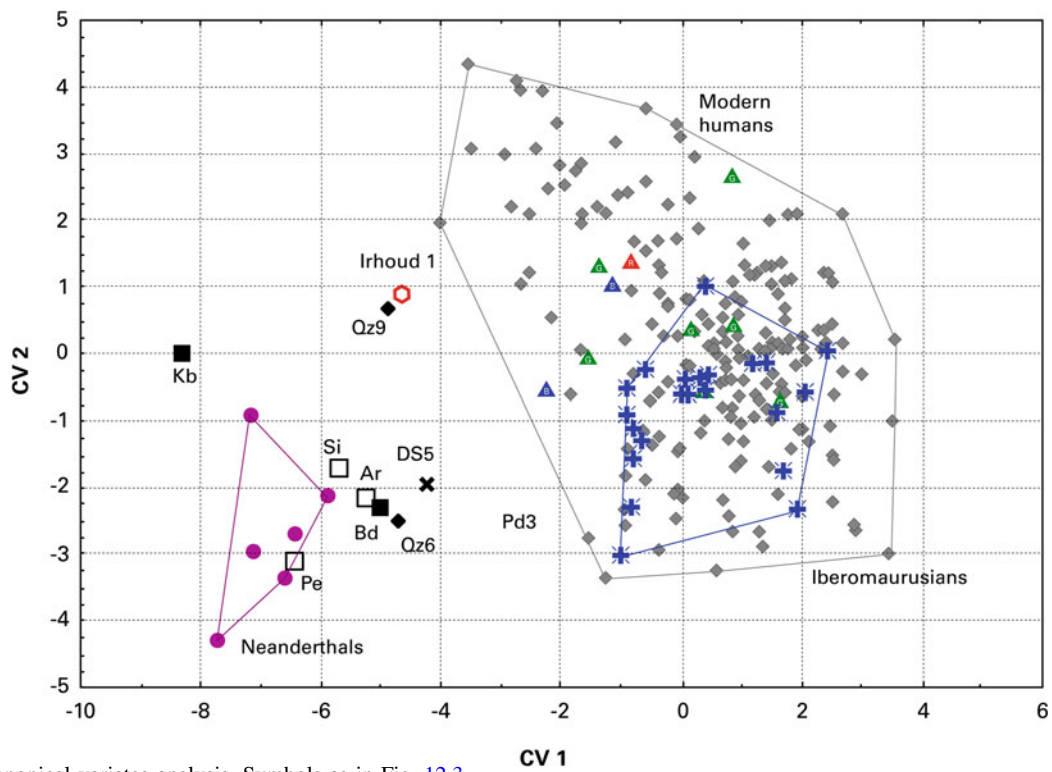


**Fig. 12.4** Canonical variates analysis. Symbols as in Fig. 12.3

**Table 12.4** Mahalanobis squared distances

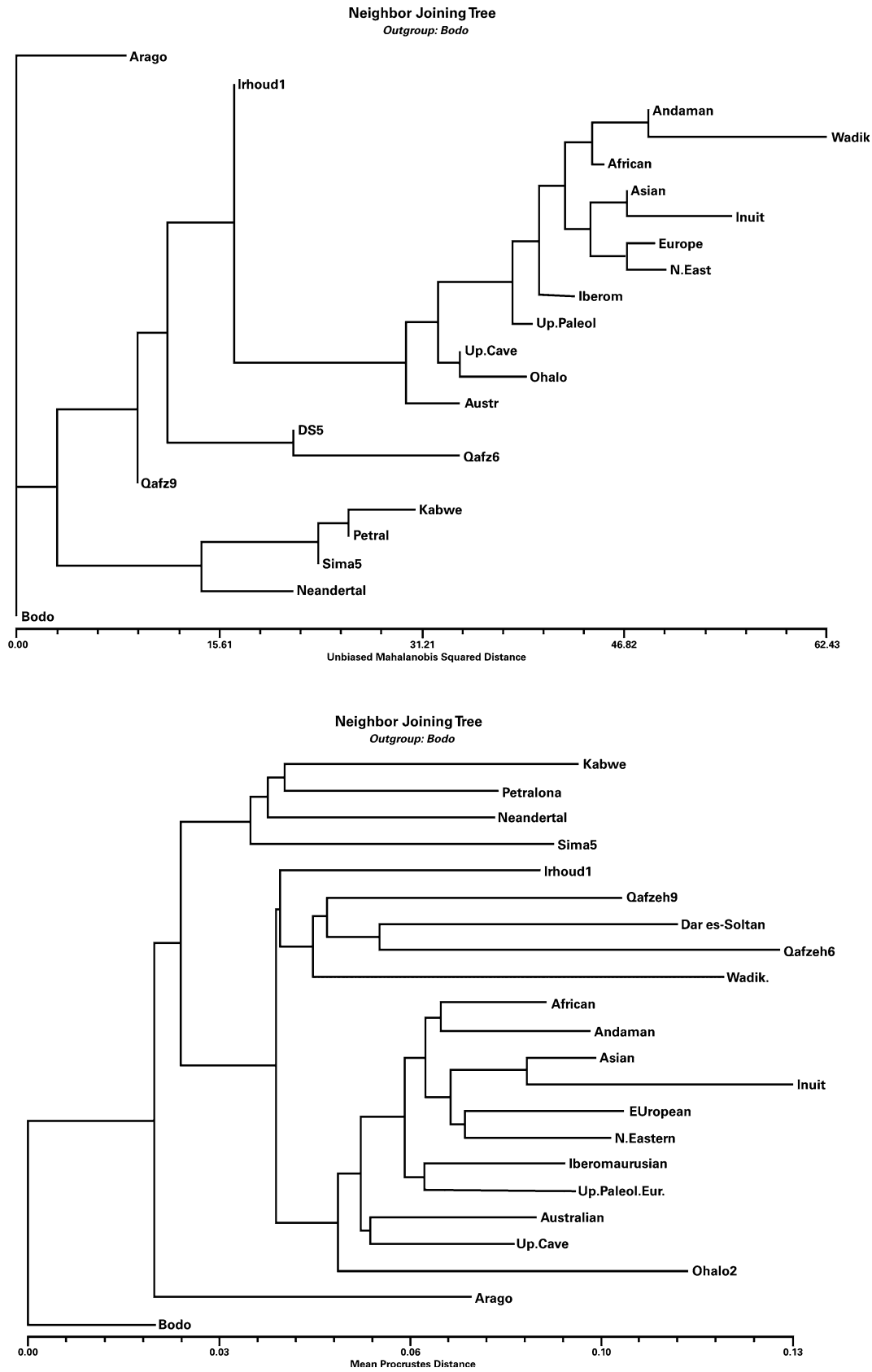
	Arago	Bodo	Irhoud I	Kabwe	Petral	Sima5	Neandertha	Andaman	African	Asian	Austr
Arago	0										
Bodo	1.53	0									
Irhoud I	17.54	9.53	0								
Kabwe	52.5	29.56	21.13	0							
Petral	24.3	3.36	16.98	-7.27	0						
Sima5	35.93	21.53	24.99	5.77	-11.5	0					
Neandertal	27.81	5.12	14.15	13.61	3.32	20.42	0				
Andaman	68.3	51.55	34.41	90.06	70.07	62.87	74.64	0			
African	64.67	40.26	23.07	69.58	54.49	56.83	63.4	5.83	0		
Asian	57.2	42.27	29.94	89.85	62.67	65.15	71.05	4.51	6.55	0	
Austr	53.07	34.84	8.44	46.88	54.24	58.67	52.2	18.25	12.78	21.45	0
DS5	<b>39.46</b>	<b>20.99</b>	<b>18.72</b>	<b>26.23</b>	<b>5.46</b>	<b>24.89</b>	<b>37.33</b>	<b>54.26</b>	<b>39.64</b>	<b>49.66</b>	<b>44.3</b>
Inuit	78.95	48.26	51.45	108.3	77.35	85.36	82.45	12.75	15.86	6.91	34
Europe	69.44	42.71	29.64	69.16	49.19	59.79	56.07	12.24	7.49	10.17	21.8
Iberom	39.08	29.64	27.63	84.88	54.15	63.55	63.07	12.28	9.28	7.23	24
Qafz6	22.07	17.7	20.67	62	38.31	55.62	39.91	71.55	71.73	60.36	57.7
Qafz9	17.1	-6.06	3.4	15.64	13.45	17.8	16.23	35.7	24.74	36.37	14
N.East	57.81	37.96	32.32	72.09	50.33	59.97	50.17	10.43	11.42	9.78	23.9
WadiK	64.54	43.63	34.26	59.44	42.57	27.79	71.94	12.11	16.65	23.63	25.2
Up.Cave	29.13	15.83	1.91	36.88	27.37	39.44	35.02	10.99	4.78	5.9	1.34
Ohalo	23.25	29.8	19.13	52.48	36.54	58.97	62	30.46	23.29	16	18
Up.Paleol	33.32	36.54	19.67	78.26	58.31	65.14	62.11	10.89	8.03	8.12	16.1

Table 12.4 (continued)

	DS5	Inuit	Europe	Iberom	Qafz6	Qafz9	N.East	WadiK	Up.Cave	Ohalo	Up.Paleol
Arago											
Bodo											
Irhoud1											
Kabwe											
Petral											
Sima5											
Neandertal											
Andaman											
African											
Asian											
Austr											
DS5	<b>0</b>										
Inuit	<b>61.3</b>	0									
Europe	<b>36</b>	13.72	0								
Iberom	<b>30.3</b>	16.59	10.48	0							
Qafz6	<b>10.7</b>	71.98	67.05	48.39	0						
Qafz9	<b>12.6</b>	53.83	36.85	26.15	16.08	0					
N.East	44.8	<b>12.49</b>	5.06	14.25	61.83	34.45	0				
WadiK	12.7	<b>39.52</b>	29.23	21.6	45.02	12.48	32.39	0			
Up.Cave	24.1	<b>15.02</b>	6.21	8.44	38.97	11.09	4.88	21.74	0		
Ohalo	23.6	<b>33.35</b>	22.96	12.18	37.8	26.38	24.97	31.7	-3.83	0	
Up.Paleol	39.2	<b>20.59</b>	14.09	4.63	55.06	27.22	10.6	27.88	1.67	9.53	0

**Table 12.5** Procrustes distances among sample mean configurations

	Kabwe	Bodo	Petralona	Arago	Sima5	Irhoud1	Neand	African	Asian	Australian	Inuit	European	Iberom	N. Eastern	Up. Pal	Ohalo2	Up. Cave	Qafzeh9	DS5	Qafzeh6	WadiK.	Andaman	
Kabwe	0.000																						
Bodo	0.125	0.000																					
Petralona	0.085	0.097	0.000																				
Arago	0.140	0.095	0.111	0.000																			
Sima5	0.108	0.112	0.086	0.113	0.000																		
Irhoud1	0.120	0.113	0.120	0.113	0.123	0.000																	
Neand	0.085	0.096	0.081	0.108	0.093	0.106	0.000																
African	0.132	0.111	0.120	0.131	0.126	0.088	0.120	0.000															
Asian	0.143	0.105	0.120	0.126	0.130	0.100	0.119	0.047	0.000														
Australian	0.117	0.115	0.121	0.127	0.129	0.078	0.118	0.053	0.073	0.000													
Inuit	0.163	0.119	0.139	0.153	0.157	0.140	0.139	0.089	0.056	0.110	0.000												
European	0.134	0.117	0.121	0.144	0.137	0.104	0.119	0.049	0.059	0.070	0.083	0.000											
Iberom	0.148	0.108	0.123	0.120	0.135	0.092	0.126	0.049	0.056	0.073	0.092	0.056	0.000										
N.Eastern	0.123	0.106	0.111	0.126	0.122	0.102	0.099	0.052	0.051	0.071	0.081	0.051	0.071	0.000									
Up.Pal	0.137	0.111	0.122	0.113	0.130	0.085	0.121	0.049	0.063	0.062	0.103	0.072	0.049	0.063	0.000								
Ohalo2	0.144	0.130	0.136	0.128	0.157	0.113	0.149	0.099	0.099	0.093	0.124	0.103	0.094	0.107	0.093	0.000							
Up. Cave	0.113	0.102	0.105	0.118	0.124	0.091	0.111	0.059	0.061	0.052	0.090	0.067	0.071	0.057	0.057	0.081	0.000						
Qafzeh9	0.113	0.113	0.118	0.120	0.119	0.095	0.102	0.102	0.116	0.097	0.153	0.121	0.113	0.107	0.105	0.135	0.106	0.000					
DS5	0.143	0.141	0.132	0.141	0.154	0.106	0.145	0.115	0.128	0.113	0.160	0.122	0.102	0.130	0.110	0.121	0.118	0.118	0.000				
Qafzeh6	0.161	0.134	0.149	0.127	0.157	0.112	0.139	0.145	0.134	0.137	0.160	0.151	0.132	0.143	0.135	0.139	0.134	0.115	0.117	0.000			
WadiK.	0.168	0.158	0.152	0.160	0.142	0.126	0.170	0.114	0.131	0.112	0.170	0.136	0.115	0.135	0.112	0.149	0.129	0.124	0.119	0.117	0.000		
Andaman	0.143	0.114	0.128	0.130	0.124	0.093	0.122	0.042	0.048	0.061	0.091	0.066	0.058	0.057	0.058	0.111	0.071	0.104	0.123	0.140	0.104	0.000	



**Fig. 12.5** Neighbor Joining Trees, based on (top) Mahalanobis  $D^2$  and (bottom) Procrustes Distances among population mean configurations. In both cases Bodo was used as an outgroup



( $d^2 = 4.63$ ). It was quite distant from all archaic fossil specimens and from Dar es-Soltan II-5 and Irhoud 1.

**PD:** The Procrustes distances among population mean configurations were calculated and reported in Table 12.5. Irhoud 1 was closest to the mean recent Australian configuration (PD = 0.078) and to the mean Upper Paleolithic European configuration (PD = 0.085). Irhoud 1 showed a rather large distance to Dar es-Soltan II-5 (PD = 0.106). Dar es-Soltan II-5 again showed larger overall distances to all other samples. The smallest distances were to the Iberomaurusian sample (PD = 0.102), and Irhoud 1 and the European Upper Paleolithic specimens (PD = 0.110). The Iberomaurusians were much closer to recent humans, and especially to the mean European Upper Paleolithic configuration (PD = 0.049).

**Cluster Analysis:** Neighbor Joining trees were built from both the Mahalanobis  $D^2$  and the Procrustes mean distances. In both instances, Bodo was used as an outgroup. The two neighbor joining trees are shown in Fig. 12.5. In both cases, Irhoud 1 and Dar es-Soltan II-5 fall, together with the Qafzeh specimens, within the modern human larger branch but as outgroups to the recent human, Upper Paleolithic, and Iberomaurusian samples. The Iberomaurusian specimens, on the other hand, are in both cases placed with the recent human groups and close to the Upper Paleolithic Europeans. The Procrustes distance tree further shows Irhoud 1, DS5, the two Qafzeh specimens, and Wadi Kubbaniya clustering together in one of the two modern human branches—the other branch comprising all recent human groups, all Eurasian Upper Paleolithic specimens, as well as the Iberomaurusian sample.

## Discussion and Conclusions

Our results indicate that the Dar es-Soltan II-5 remains do not show strong morphological similarities to the later Iberomaurusian population. Although this specimen is clearly a modern human, it seems more similar to the early anatomically modern humans from Qafzeh, to the Late Pleistocene North African specimen from Wadi Kubbaniya, and also to the earlier Moroccan specimen Jebel Irhoud 1. Some level of regional continuity is suggested by the Procrustes distance analysis, where Dar es-Soltan II-5 was found to be closest to the Iberomaurusian sample and to Jebel Irhoud 1. However, these distances were very large (approximately double the distances among neighboring recent human populations like the European and near eastern samples), and do not seem to us to imply a close relationship between Dar es-Soltan II-5 and either the Jebel Irhoud individual or the Iberomaurusian sample. Keeping in mind the caveats inherent in the comparative analysis of a single specimen, the overall large Procrustes distances of Dar es-Soltan II-5 to all samples and

its similarities to Late Pleistocene specimens in the PCA, CVA, and in both Mahalanobis and Procrustes distances suggest to us that a characterization as an early modern human is the most appropriate for this specimen.

Our findings are consistent either with an evolutionary discontinuity between the Aterian and the later Iberomaurusian populations, or with a large chronological period between these two samples. As such, they are also consistent with the recent dating results suggesting that the Dar es-Soltan II Aterian human remains could be placed ca. 80 ka (Raynal and Occhietti 2012). The Iberomaurusian remains, on the other hand, show strong morphological similarities with the European Upper Paleolithic sample used here. This result supports previous suggestions that the two groups might have shared a common population history (Ferembach 1962, 1985).

Our analysis supports an earlier chronology and taxonomic placement of Dar es-Soltan II-5 with early anatomically modern humans, as well as affinities between the Upper Paleolithic peoples of Europe and those of the somewhat later Moroccan Iberomaurusians. However, it must be noted that this study did not address the issue of allometry, which has been documented to affect facial morphology in important ways (Rosas and Bastir 2002, 2004; Strand-Viðarsdóttir et al. 2002; Maddux and Franciscus 2008). Such allometric effects may account for some of our unexpected results, such as the small Mahalanobis  $d^2$  distance between Dar es-Soltan 5 and Petralona (Table 12.4). Analysis of size-related effects would help clarify these results. Finally it should be kept in mind that the face has previously been argued not to be phylogenetically as informative as other parts of the cranium (e.g., Harvati and Weaver 2006a, b). Analysis of other anatomical regions, such as the cranial vault and base and the dental morphology, will help resolve the issues explored here more conclusively.

**Acknowledgments** We thank all curators for access to fossil and recent human skeletal collections. Special thanks go to the Direction de l'INSAP (Royaume du Maroc), Direction du Patrimoine, Ministère de la Culture (Royaume du Maroc), Monsieur le Conservateur du Musée Archéologique de Rabat, and Prof. Henry de Lumley (Institut de Paléontologie Humaine) for allowing access to the Jebel Irhoud, Dar es-Soltan, and Iberomaurusian material. Comments provided by two anonymous reviewers helped to greatly improve the manuscript. This research was supported by the Max-Planck Society and the EVAN Marie Curie Research Training Network MRTN-CT-019564. NYCEP morphometrics contribution No. 35.

## References

- Bastir, M., & Rosas, A. (2004). Facial heights: Evolutionary relevance of postnatal ontogeny for facial orientation and skull morphology in humans and chimpanzees. *Journal of Human Evolution*, 47, 359–381.
- Bouzouggar, A., Barton, R. N. E. (2012). The identity and timing of the Aterian in Morocco. In J.-J. Hublin & S. McPherron (Eds.), *Modern origins: A North African perspective*. Dordrecht: Springer.
- Debénath, A. (1976). Le site de Dar es-Soltan 2, à Rabat (Maroc). *Bulletin et Mémoires de la Société d'Anthropologie de Paris*, 3, 181–182.

- Debénath, A., Raynal, J.-P., Roche, J., Texier, J.-P., & Ferembach, D. (1986). Stratigraphie, habitat, typologie et devenir de l'Atérien Marocain: Données récentes. *L'Anthropologie*, 90, 233–246.
- Ferembach, D. (1962). *La nécropole épipaléolithique de Taforalit (Maroc Oriental). Étude des squelettes humains. Avec la collaboration de J. Dastugue et M. J. Poitrat-Targowla*. Casablanca: Edita.
- Ferembach, D. (1976). Les restes humains de la grotte de Dar es-Soltan 2 (Maroc), campagne 1975. *Bulletins et Mémoires de la Société d'Anthropologie de Paris*, 3, 183–193.
- Ferembach, D. (1985). On the origin of the Iberomaurusians (Upper Paleolithic: North Africa). A new hypothesis. *Journal of Human Evolution*, 14, 393–397.
- Gunz, P., & Harvati, K. (2007). The Neanderthal 'chignon': Variation, integration and homology. *Journal of Human Evolution*, 52, 262–274.
- Harvati, K. (2001). *The Neanderthal problem: 3D geometric morphometric models of cranial shape variation within and among species*. Ph.D. dissertation, City University of New York.
- Harvati, K. (2003a). Quantitative analysis of Neanderthal temporal bone morphology using 3-D geometric morphometrics. *American Journal of Physical Anthropology*, 120, 323–338.
- Harvati, K. (2003b). The Neanderthal taxonomic position: Models of intra- and inter-specific craniofacial variation. *Journal of Human Evolution*, 44, 107–132.
- Harvati, K., & Weaver, T. D. (2006a). Reliability of cranial morphology in reconstructing Neanderthal phylogeny. In K. Harvati & T. Harrison (Eds.), *Neanderthals revisited: New approaches and perspectives* (pp. 239–254). Dordrecht: Springer.
- Harvati, K., & Weaver, T. D. (2006b). Human cranial anatomy and the differential preservation of population history and climate signatures. *Anatomical Record*, 288A, 1225–1233.
- Hublin, J.-J. (1985). Human fossils of the North African Middle Pleistocene and the origin of *Homo sapiens*. In E. Delson (Ed.), *Ancestors: The hard evidence* (pp. 283–288). New York: Alan R. Liss.
- Hublin, J.-J. (1992). Recent human evolution in northwestern Africa. In M. Aitken, P. Mellars, C. B. Stringer (Eds.), *The origin of modern humans, the impact of science-based dating. Philosophical Transactions of the Royal Society B*, 337, 185–191.
- Hublin, J.-J. (2001). Northwestern African Middle Pleistocene hominids and their bearing on the emergence of *Homo sapiens*. In L. Barham & K. Robson-Brown (Eds.), *Human roots. Africa and Asia in the Middle Pleistocene* (pp. 99–121). Bristol: CHERUB, Western Academic and Specialist Press Ltd.
- Marcus, L. F. (1993). Some aspects of multivariate statistics for morphometrics. In L. F. Marcus, E. Bello, & A. García-Valdecasas (Eds.), *Contributions to morphometrics* (pp. 99–130). Madrid: Monografias Museo Nacional de Ciencias Naturales.
- Mardia, K. V., & Bookstein, F. L. (2000). Statistical assessment of bilateral symmetry of shapes. *Biometrika*, 87, 285–300.
- Maddux, S. D., & Franciscus, R. G. (2008). Allometric scaling of infraorbital surface topography in *Homo*. *Journal of Human Evolution*, 56, 161–174.
- Nicholson, E., & Harvati, K. (2006). Quantitative analysis of human mandibular shape using 3-D geometric morphometrics. *American Journal of Physical Anthropology*, 131, 368–383.
- O'Higgins, P. (2000). The study of morphological variation in the hominid fossil record: Biology, landmarks and geometry. *Journal of Anatomy*, 197, 103–120.
- Raynal, J.-P., Occhietti, S. (2012). Amino-chronology and an earlier age for the Aterian. In J.-J. Hublin & S. McPherron (Eds.), *Modern origins: A North African perspective*. Dordrecht: Springer.
- Richter, D., Moser, J., Nami, M. (2012). New data from the site of Ifri n'Ammar (Morocco) and some remarks on the chronometric status of the Middle Paleolithic in the Maghreb. In J.-J. Hublin & S. McPherron (Eds.), *Modern origins: A North African perspective*. Dordrecht: Springer.
- Rohlf, F. J., & Marcus, L. F. (1993). A revolution in morphometrics. *Trends in Ecology & Evolution*, 8, 129–132.
- Rosas, A., & Bastir, M. (2002). Thin-plate spline analysis of allometry and sexual dimorphism in the human craniofacial complex. *American Journal of Physical Anthropology*, 117, 236–245.
- Rosas, A., & Bastir, M. (2004). Geometric morphometric analysis of allometric variation in the mandibular morphology from the hominids of Atapuerca, Sima de los Huesos Site. *The Anatomical Record Part A*, 278A, 551–560.
- Strand-Viðarsdóttir, U., O'Higgins, P., & Stringer, C. (2002). A geometric morphometric study of regional differences in the ontogeny of the modern human facial skeleton. *Journal of Anatomy*, 201, 211–229.
- Smith, T. M., Tafforeau, P., Reid, D. J., Grün, R., Eggins, S., Boutaiout, M., et al. (2007). Earliest evidence of modern human life history in North African early *Homo sapiens*. *Proceedings of the National Academy of Sciences of the USA*, 104, 6128–6133.